Outracing Lung Signal Decay – Potential of Ultrashort Echo Time MRI

Dem Signalzerfall in der Lunge zuvorkommen – Potenzial der Ultrashort-Echo-Time-MRT

Authors

Mark Oliver Wielpütz[1, 2, 3], Simon M. F. Triphan[1, 2, 3], Yoshiharu Ohno[4], Bertram J. Jobst[1, 2, 3], Hans-Ulrich Kauczor[1, 2, 3]

Affiliations

1 Department of Diagnostic and Interventional Radiology, Subdivision of Pulmonary Imaging, University Hospital of Heidelberg, Heidelberg, Germany
2 Translational Lung Research Center Heidelberg (TLRC), German Lung Research Center (DZL), Heidelberg, Germany
3 Department of Diagnostic and Interventional Radiology with Nuclear Medicine, Thoraxklinik at the University Hospital of Heidelberg, Heidelberg, Germany
4 Advanced Biomedical Imaging Research Center, Kobe University Graduate School of Medicine, Kobe, Japan

Key words

ultrashort TE, lung imaging, functional lung imaging, lung MRI

received 22.05.2018
accepted 13.08.2018

Bibliography

DOI https://doi.org/10.1055/a-0715-2246
Published online: 26.9.2018
Fortschr Röntgenstr 2019; 191: 415–423

ISSN 1438-9029

Correspondence

Herr PD Dr. Mark Oliver Wielpütz
Diagnostic and Interventional Radiology, University Hospital of Heidelberg, Im Neuenheimer Feld 110, 69120 Heidelberg, Germany
Tel.: ++ 49/62 21/56 64 10
Fax: ++ 49/62 21/56 57 30
mark.wielpuetz@med.uni-heidelberg.de

ZUSAMMENFASSUNG

Hintergrund Die Herausforderungen der Magnetresonanztomografie (MRT) des Lungenparenchyms liegen in der Herz- und Atembewegung der Patienten, niedrigen Protonendichte und vor allem dem extrem schnellen Signalabfall. Dieser entsteht durch die für den Gasaustausch optimierte Lungenstruktur.

Methoden Diese Übersicht basiert auf systematischer Literaturrecherche sowie jährlicher Teilnahme an Konferenzen zum Thema Lungen-MRT über mehr als 20 Jahre durch mindestens einen Autor.

Ergebnisse und Schlussfolgerung Das Problem der Bewegung wurde durch Entwicklungen wie Triggering, Gating und parallele Bildgebung angegangen. Das Problem der geringen Protonendichte hat sich bei Krankheiten, die zu einer Zunahme an Gewebedichte und damit Signal relativ zum Hintergrund, teilweise als Vorteil erwiesen. Um den Signalabfall auszugleichen, wurden ultrashort-echo-time (UTE)-Methoden entwickelt, um die Zeit zwischen Anregung und Auslese zu minimieren. Während diese bereits vor längerer Zeit postuliert wurden, erlauben verbesserte Scanner-Hard- und -Software jetzt Echozeiten unterhalb von 200µs und damit ein signifikant höheres Signal aus der Lunge. Indem man so dem Signalabfall zuvorkommt, lässt sich das Signal der wenigen verfügbaren Protonen effizienter ausnutzen. Solche UTE-Techniken können nicht nur die morphologische Bildgebung in der Lunge verbessern, sondern auch die Möglichkeiten der funktionellen Bildgebung erweitern, einschließlich Ventilations- und Perfusions-Bildgebung sowie der Quantifizierung anderer Parameter. Dem wachsenden Fortschritt in der Lungen-MRT folgend, zeigt diese Übersicht technische Möglichkeiten und liefert einen Überblick über aufkommende Anwendungen am Menschen bzw. Krankheiten. Diese zeigen, dass die UTE-MRT in naher Zukunft eine wichtige Rolle in der morphologischen und funktionellen bildgestützten Untersuchung der Lunge spielen wird.

Kernaussagen:

- Ultrashort-echo-time (UTE)-MRT ist auf modernen Scannern technisch machbar und verfügbar.
- UTE-MRT erlaubt CT-artige Bildqualität für die morphologische Darstellung der Lunge.
- Vorläufige Studien zeigen Verbesserungen gegenüber konventionellen Echozeiten für die morphologische Bildgebung von Lungenkrebs und Atemwegserkrankungen.
- UTE-MRT könnte die Sensitivität funktioneller Prozesse wie Perfusionsquantifizierung und Gewebscharakterisierung erhöhen.

ABSTRACT

Background Magnetic resonance imaging (MRI) of the pulmonary parenchyma is generally hampered by multiple challenges related to patient respiratory- and circulation-related motion, low proton density and extremely fast signal

decay due to the structure of the lungs evolved for gas exchange.

Methods Systematic literature database research as well as annual participation in conferences dedicated to pulmonary MRI for more than the past 20 years by at least one member of the author team.

Results and Conclusion The problem of motion has been addressed in the past by developments such as triggering, gating and parallel imaging. The second problem has, in part, turned out to be an advantage in those diseases that lead to an increase in lung substance and thus an increase in signal relative to the background. To reduce signal decay, ultrashort echo time (UTE) methods were developed to minimize the time between excitation and readout. Having been postulated a while ago, improved hardware and software now open up the possibility of achieving echo times shorter than 200 µs, increasing lung signal significantly by forestalling signal decay and more effectively using the few protons available. Such UTE techniques may not only improve structural imaging of the lung but also enhance functional imaging, including ventilation and perfusion imaging as well as quantitative parameter mapping. Because of accelerating progress in this field of lung MRI, the review at hand seeks to introduce some technical properties as well as to summarize the growing data from applications in humans and disease, which promise that UTE MRI will play an important role in the morphological and functional assessment of the lung in the near future.

Key Points:

- Ultrashort echo time MRI is technically feasible with state-of-the-art scanner hardware.
- UTE MRI allows for CT-like image quality for structural lung imaging.
- Preliminary studies show improvements over conventional morphological imaging in lung cancer and airways diseases.
- UTE may improve sensitivity for functional processes like perfusion and tissue characterization.

Citation Format

- Wielpütz MO, Triphan SM, Ohno Y et al. Outracing Lung Signal Decay – Potential of Ultrashort Echo Time MRI. Fortschr Röntgenstr 2019; 191: 415–423

Introduction

Structural lung imaging with MRI is hampered by the limited presence of protons per volume and very short T2* relaxation times of normal lung tissue [1]. This has led to the spin density-driven classification of "plus" and "minus" pathologies in the lung. The former can be identified easily before the low signal background of the lung in conventional pulse sequences due to a disease-related increase in tissue, fluid or cells in the alveolar space, pulmonary interstitium incl. airway wall, vasculature or pleural space, with a concomitant increase in protons [2 – 4]. This fact has spawned a multitude of studies on the use of MRI in such diseases, e. g. leading to the introduction of MRI into routine patient care in lung cancer or cystic fibrosis, mostly as an alternative to CT [2, 5, 6]. The latter disease group has remained a great challenge in lung MRI due to a loss in tissue or vasculature with a subsequent increase in airspace, limiting its use in emphysema, cysts and pneumothorax [3, 4]. Since the challenge posed by short T2* has been known, the concept of using ultrashort echo times to compensate for this has been postulated [1, 7] soon after these methods were demonstrated [8, 9]. Quick readouts after excitation with an echo time of less than 200 µs could forestall the extremely short T2* and the respective fast signal decay in (healthy) lung tissue, and thereby increase the detection of "minus pathologies", termed ultrashort echo time (UTE) imaging. Various technical challenges had to be overcome to make UTE imaging effective in the lungs: Breathing motion has to be compensated for and the low proton density of only 20 % to 35 % relative to other tissues [10] poses an additional difficulty. An additional problem is the very large field of view required for lung imaging. Apart from this, most challenges for the application of UTE are of a technical nature, such as scanner dead-times as well as gradient distortions and delays. As the intrinsic dead-time of the MR scanner limits the minimum TE, UTE methods have only become practical fairly recently, as these problems were solved.

Investigators studied UTE for structural as well as for functional imaging, e. g. lung perfusion as well as quantitative readouts of lung relaxation times. The present review provides an introduction into the technical challenges and their current solutions in UTE imaging of the lung, as well as an overview of the preliminary results of initial clinical studies.

Motivation for the use of UTE in the lungs

Susceptibility effects in lung tissue

Boundary surfaces between volumes with different magnetic susceptibilities χ produce local magnetic gradients due to the different local fields on both sides of the boundary (▶ **Fig. 1**). In the lungs, tissue made up of blood vessels as well as extracellular space and the gas in the alveoli represent just such volumes with very different χ. Since the lungs are responsible for the gas exchange, they naturally contain a very large number of such boundary surfaces. Since any field gradient introduces locally varying Larmor frequencies, it leads to dephasing of spins which is felt as an exponential decay of signal with the time coefficient T2'. $T2^* = 1/(1/T2' + 1/T2)$ is the effective transverse relaxation time, made up of T2, which is determined by microscopic structure and much more commonly used as a source of contrast in MRI, and T2' which results from mesoscopic gradients like those generated by lung structure. While in other tissues it would be short T2 times that mandate the use of UTE sequences, in the lungs T2* is far more dominant, while T2 has been measured to be around 70 ms [11]. Thus, the T2* relaxation time in the lungs

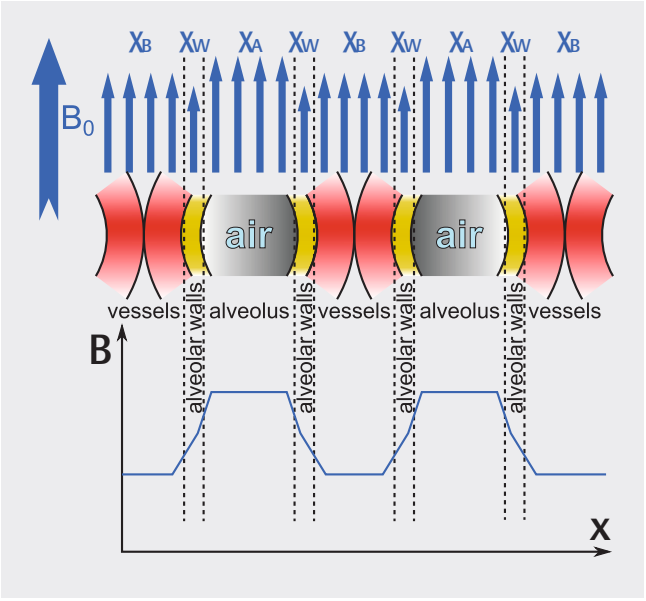

▶ **Fig. 1** Diagram illustrating the susceptibility effects in the lung parenchyma: χA in air is dominated by oxygen and slightly positive, while χB in blood and χW in remaining lung water are strongly negative, leading to local gradients at the boundaries. There are many such interfaces between these volumes in every voxel.

▶ **Abb. 1** Suszeptibilitätseffekte im Lungenparenchym: χA in der Luft wird durch Sauerstoff beherrscht und ist daher leicht positiv, während χB im Blut und χW im übrigen Lungenwasser deutlich negativ ist, was zu starken lokalen Gradienten an den Grenzflächen führt. In jedem Voxel existieren viele solcher Grenzflächen.

is extremely short, on the order of 1 – 2 ms at 1.5 T [10, 12, 13]. Since a large amount of signal, which is already precious due to the low proton density in the lungs, is lost to T2* decay when acquiring images at conventional echo times, UTE sequences are particularly desirable in lung imaging.

Respiratory motion

An additional intrinsic challenge of lung imaging is the need to account for breathing motion. For conventional MRI sequences, it is possible, mainly by utilizing parallel imaging techniques, to complete an entire acquisition within the duration of one breath-hold, even when the patient's capacity for breath-holding is impaired [14]. Due to the relatively long acquisition times required to acquire full 3 D k-spaces in UTE sequences (around 8 – 10 min. [15]), this is generally difficult. However, breath-hold measurements have been demonstrated using extremely short repetition times in combination with gradient compensations to account for gradient delays [16].

Otherwise, some form of navigation during free breathing is advisable. Luckily, the radial acquisition schemes used for UTE are well-suited for self-gating (or 'dc'-gating) since every projection already contains the k-space center. By this approach, the need for extrinsic triggering devices and the negative impact on image quality of usual navigator echoes used to monitor diaphragmatic motion are avoided, although device triggers are also well-suited for gating radial data. When doing so, the radial acquisition scheme is still beneficial due to the oversampling of the central k-space. This means that images are generally robust against motion, which will lead to blurring at worst rather than ghosting artifacts like in Cartesian encoding, and can be assembled from arbitrarily selected projections. Alternatively, the radial readout can be exploited to actually reconstruct low-resolution images dynamically and then detect the motion of the diaphragm over time in these, allowing for image-based self-gating [17]. The intrinsic signal variation of a dedicated second echo in a dual echo radial 3 D UTE acquired in shallow free breathing can also be used to retrospectively separate two sets of images in inspiration and expiration [18], effectively gating using T_2^*.

Finally, gating causes consecutive projections to be discarded for reconstruction. Due to this, the order and spatial distribution of projections is especially important when employing any kind of gating. Different sampling strategies have been investigated to minimize artifacts caused by gaps in k-space [17, 19].

Technical basis and types of UTE sequences

To measure the MR signal at an ultrashort echo time, the signal readout must start immediately after the excitation in the center of k-space. Accordingly, there are essentially two prerequisites for UTE imaging: The excitation must be performed in such a way that the signal can be read immediately after the center is reached in excitation k-space, and the readout must begin immediately in the center of acquisition k-space. The differences in the UTE variants below lie mainly in how these prerequisites are achieved. It should also be noted that (contrary to what the names chosen for methods might imply) the essential limitation of echo time is always the dead-time of the scanner hardware in use. As the radio frequency amplifiers necessarily require some time to switch from transmit to receive mode, the actual TE can never be shorter than this dead-time. Accordingly, all methods mentioned here have the shortest TE they can achieve, which is not only determined by the method itself but also by the scanner type used. Generally, these methods depend much more on the capabilities of scanner hardware and software than conventional MRI sequences. Due to the adaptations to MR excitation used to achieve UTE, all described methods are necessarily gradient echo (GRE) sequences, which are commonly referred to as 'T1-weighted' sequences, the difference with respect to conventional GREs being that T2* weighting can be reduced drastically. For the imaging of the lung pathologies mentioned above, favoring pure proton density contrast over T1 weighting may however be sensible and is most often employed in the work presented in this review.

3 D UTE

In the 3 D UTE sequence (▶ **Fig. 2a**), the time after the excitation is minimized by using a completely unmodulated, 'hard' block pulse [20]. While this allows for a very short pulse duration, on the order of a few tens of microseconds, the lack of frequency modulation also prevents slice selection. Accordingly, all protons in the scanner's main field will be excited and need to be encoded.

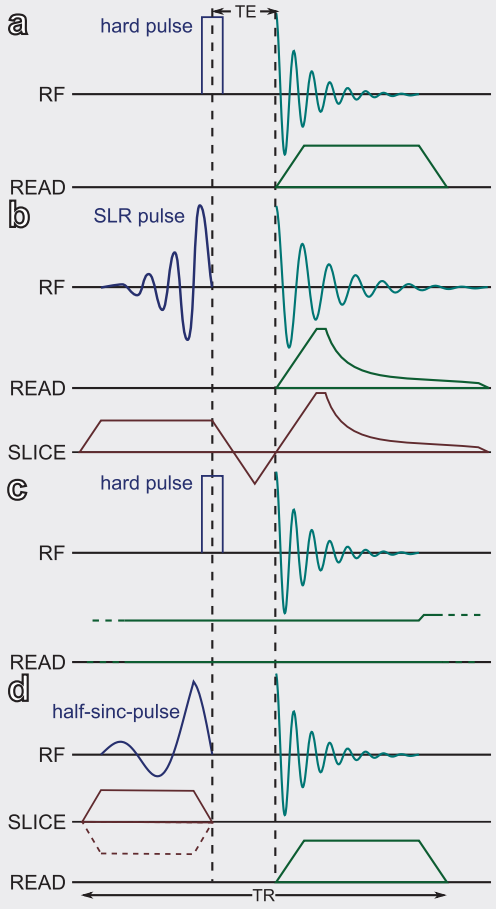

▶ **Fig. 2** Basic pulse sequences of UTE sequences. Note that the width of pulse objects shown here is not indicative of their duration in a practical sequence: In UTE sequences, the duration of rectangular pulses and TE itself are far shorter than the read gradients and other RF pulses shown here and would not be visible in the diagram. **a** 3 D UTE utilizes a hard, nonselective pulse and a center-out, ramp-sampling readout. **b** Improved 3 D UTE sequence including Shinnar-LeRoux pulses and arc-length optimized readout gradients. **c** In ZTE, the readout gradient is already active during the excitation pulse and only needs slight adjustment before the next excitation. **d** In 2 D UTE, the excitation is done twice using a half-pulse, reversing the polarity of the slice select gradient in the second measurement. Note that spoiler gradients at the end of TR have been omitted for readability and that for all methods, double or multi-echo variants are often used.

▶ **Abb. 2** Grundlegende UTE-Pulssequenzen. Die Länge der gezeigten Pulse entspricht nicht den tatsächlichen Verhältnissen: In UTE-Sequenzen sind Rechteckpulse und TE selbst sehr viel kürzer als die Auslesegradienten und wären in einer Zeichnung nicht sichtbar. **a** 3D-UTE verwendet einen harten, nicht selektiven Puls und eine Auslese, die im k-Raum-Zentrum und auf der Rampe des Auslesegradienten beginnt. **b** Verbesserte 3D-UTE-Sequenz, die Shinnar-LeRoux-Pulse und Bogenlänge-optimierte Auslesegradiente verwendet. **c** In ZTE ist der Auslesegradient bereits während des Anregungspulses aktiv und erfordert nur eine leichte Anpassung vor der nächsten Anregung. **d** In der 2D-UTE wird die Anregung 2-mal mittels eines Halbpulses ausgeführt, wobei die Polarität des Schichtauswahlgradienten für die zweite Messung umgekehrt wird. Spoiler-Gradienten wurden im Interesse der Lesbarkeit weggelassen. Für alle diese Methoden sind außerdem Doppel- und Multi-Echovarianten üblich.

To fulfil the second condition, the signal is read out going from the center of k-space moving outward in a radial trajectory. Since a phase-encoding gradient would prolong TE by its duration and no slice encoding is possible, this radial frequency encoding must be performed in three dimensions. Additionally, since gradient switching is not instantaneous, the frequency encoding gradient needs some time to rise to its full amplitude (the ramp time). To begin the readout immediately, sampling must necessarily include the gradient ramp. This entails several disadvantages: While the theoretical shape of the gradient is trapezoidal, the actually applied gradient shape may diverge from this, resulting in a distorted image. Mainly, these divergences consist of gradient delays, where the starting time of the gradient is incorrect, and eddy currents, which distort the actual shape of the ramp. Gradient delays are common to other radial acquisition methods as well but can be measured and corrected for. To account for gradient shape distortions, it is necessary to measure the actual trajectory through k-space produced by the gradients and then use this result for the reconstruction of images [21]. However, this requires a separate measurement for each set of resolution, field of view and bandwidth parameters, per scanner.

Another disadvantage of the fully asymmetric radial readout is sampling inefficiency due to non-uniform sampling. For a readout with a plain trapezoidal gradient, this results in an SNR loss of roughly 25 %. To compensate for this, arc length-optimized gradients have been introduced [15], minimizing the time spent in inner k-space. These very dynamic gradients exacerbate the problems with eddy currents and delays described above, increasing the importance of trajectory measurements. In order to enable a slab-selective excitation, it has further been proposed to replace block pulses with minimum-phase Shinnar-LeRoux (SLR) pulses [15] designed specifically to account for the decay of signal during excitation (▶ **Fig. 2b**).

ZTE

Zero TE (ZTE) sequences [22 – 24] were developed to circumvent the problems caused by eddy currents and gradient delays. When using a 3 D UTE excitation based on unmodulated hard pulses to allow for extremely fast pulses, no slice selection is possible. However, this can be used to one's advantage: Eddy currents cannot be prevented while switching gradients, but as no slice select gradient is needed, the readout gradients can be switched on before the pulse is given, starting the readout immediately after the excitation on an entirely flat gradient (▶ **Fig. 2c**). The price for this is that during the unavoidable dead-time the readout already leaves the k-space center. Thus, the points in the absolute center have to be acquired in a different manner. In the original ZTE method, this gap in k-space is completed using algebraic reconstruction, extrapolating from the surrounding acquired points. Since this is only possible if the gap is small, the scanner's dead-time is a major limiting factor for this approach.

An alternative way to fill the gap in the k-space center has been implemented in the PETRA sequence (Siemens AG, Erlangen, Germany) [25, 26], where almost the entire k-space is read using ZTE, but the innermost points are separately acquired using single-point measurements [27] afterwards. In theory, it would also be

possible to acquire the entire k-space as single points to minimize TE everywhere in k-space, but this is relatively time-consuming.

ZTE-based sequences are comparable in terms of the time needed for encoding k-space to ramp-sampling 3 D UTE methods, but have an additional advantage, i. e., readout gradients do not have to be switched off but can rather be merely slightly adjusted after each readout to achieve the 3 D angle for the next projection, if the angle ordering is chosen accordingly. Therefore, the change in encoding gradient and thus physical strain on the gradient coils is minimal, which results in an extremely quiet acquisition [25]. As ZTE does not continuously acquire the k-space center, it cannot exploit this for easy dc-gating as in 2 D or 3 D UTE. The essentially radial encoding is, however, still well suited for navigating using respiratory bellows or similar approaches.

2 D UTE

If the time to acquire a full 3 D k-space is not available, it is possible to exploit the linearity of slice excitation rather than using hard pulses [9]. Since, for low flip angles, the slice profile is approximately the Fourier transform of the pulse profile and the transform is linear, exciting and subsequently measuring with all parts of a pulse and summing the resulting signals is equivalent to only exciting with the complete pulse. Thus, by exciting with two halves of a pulse ending in the center of excitation k-space, the TE can also be minimized [28]. When using a sinc-shaped pulse, (sinc(x) = sin(x)/x) is the Fourier transform of a plain rectangular slice profile. This can be achieved by using the first half of the pulse in one TR and then repeating the measurement with the polarity of the slice selection gradient reversed (▶ **Fig. 2 d**). Since this reverses the direction of the k-space trajectory, it will cover the opposite side of excitation k-space, again ending in the center. While this allows for the acquisition of 2 D slices covering k-space much faster than isotropic 3 D volumes, every projection has to be acquired twice. While this was the first UTE method applied in the lungs [7], 3 D methods have been adapted at a faster rate recently. Nevertheless, the 2 D UTE approach is useful for dynamic acquisitions, e. g. for parameter quantification [29]. These methods can be combined as necessary: For example, half-sinc pulses can be used to excite a large slab, followed by radial 3 D encoding, combining aspects of the 2 D and 3 D UTE.

Potential applications in lung disease

Morphological Imaging with UTE

MRI of lung nodules, airway and interstitial lung diseases (“plus pathologies”) will obviously benefit from the higher resolution of UTE acquisitions along with a reduction of susceptibility artifacts. Lung signal intensity with a 3 D UTE on a clinical 3 T system in healthy mice at different lung volumes correlates well with lung tissue density [30], which is an important prerequisite for structural and functional imaging. The SNR was roughly twice as high at an echo time of 100 µs compared to 800 µs. Similar results were found in healthy volunteers with the SNR depending on respiratory state [31]. The following subsection introduces the most promising recent advances in the application of UTE-MRI in clinical imaging.

Nodule Detection and Characterization

Conventional MR sequences at 1.5 T may detect nodules down to a diameter of 4 mm in an *ex vivo* setting [32], while in the setting of lung cancer screening a somewhat weaker overall sensitivity of 48 % and a specificity of 88 % in comparison to low-dose CT for lesions averaging 15 mm in diameter was found [33]. In contrast, a sensitivity of 82 % was reported with a free-breathing UTE acquisition in 82 nodules > 4 mm in 8 patients [34]. When thin-section UTE was compared to CT in a group of 63 patients with 243 nodules, the sensitivity and specificity were 93 % and 99 %, respectively, for UTE as well as CT. In addition, inter-observer (κ = 0.94 – 0.95) and inter-method (κ = 0.98 – 0.99) agreement for differentiation between subsolid, part-solid and solid nodules was very high [35]. Moreover, the characterization of malignant nodules with UTE is highly concordant with CT with high inter-reader agreement also similar to CT [36].

Neonatal Lung Disease

Another exciting application of the improved resolution is monitoring early lung disease in neonates and preschool children, e. g. bronchopulmonary dysplasia (“minus pathology”) using a dedicated small-bore neonate scanner [38]. UTE achieved a higher parenchymal signal and fewer motion artifacts compared to a 3 D fast gradient recalled echo sequence in ten free-breathing non-sedated infants. The visibility of central airways in 37 infants (23 – 43 gestational weeks) at 3 T using PETRA was good in 90 % of the main airways, but only 22 % for the right upper lobe bronchus [39].

Obstructive Airway Diseases

In cystic fibrosis (CF), patients develop air-trapping due to mucus obstruction and progressive bronchiectasis due to chronic inflammation [40]. Proton MRI including contrast-enhanced perfusion imaging depicts morphological changes of the CF lung similar to CT including an MRI scoring system [41, 42], and is even capable of showing the full spectrum of disease severity in newborns and therapy response in acute exacerbation [6, 43, 44]. UTE may deliver structural images for the detection and scoring of bronchiectasis comparable to CT [25]. The increase in resolution may also improve chances for quantitative post-processing of structural changes and functional assessment. In COPD, which is generally characterized by a limited differentiation of emphysema from normal lung tissue due to the low proton density (“minus pathology”), UTE also identified emphysema and bullae in high agreement with CT (κ = 0.75 – 0.78) in 85 patients [37] (▶ **Fig. 3, 4**). This also applies to the thin walls of cystic changes as found in honeycombing [3], which are otherwise not visible on conventional MRI sequence due to lower resolution and susceptibility artifacts at the air-tissue interfaces (▶ **Fig. 4**). Here, UTE-MRI achieved an agreement of κ = 0.83 with CT for the assessment of honeycombing [37].

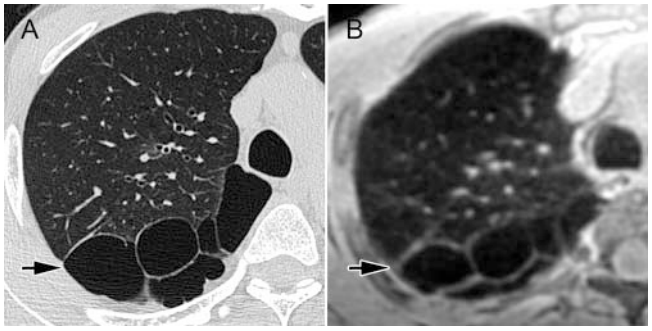

▶ **Fig. 3** 58-year-old male with large thin-walled bullae of the right apical lung on CT **A** and on 3 D respiratory-gated pulmonary thin-section MR imaging with UTE at 96 µs on a 3 T system **B**. A clear difference in the signal for air inside bullae and lung parenchyma itself can be seen, demonstrating UTE's higher signal output for normal lung in comparison to conventional MRI pulse sequences. Note that UTE MRI is reconstructed in the end-expiration phase.

▶ **Abb. 3** 58 Jahre alter Mann mit großen, dünnwandigen Bullae in der rechten apikalen Lunge, sichtbar im CT **A** und in der Dünnschicht-3D-UTE mit Atemgating, aufgenommen bei 96µs auf einem 3T-Scanner **B**. Ein deutlicher Signalunterschied innerhalb der Bullae und dem Lungenparenchym selbst ist sichtbar, wodurch sich das im Vergleich zu konventionellen Sequenzen höhere Parenchym-Signal in der UTE zeigt. Die UTE-Messung wurde in Exspiration rekonstruiert.

Functional imaging using UTE and potential clinical applications

Oxygen-enhanced imaging

Due to the paramagnetic attributes of molecular oxygen (O_2), increasing the concentration of O_2 in the breathing gas reduces T1 in the lungs locally when it dissolves. This has been exploited to make local ventilation visible by observing signal enhancement induced by T1 reduction [45]. However, since T2* in the lungs is determined by the susceptibility difference between gas and tissue, an increased concentration of oxygen also further reduces T2*[46]. Thus, in combination with the already very short T2*, the use of a UTE sequence is especially desirable for oxygen-enhanced lung imaging [29, 47]. An oxygen-enhanced 3 D UTE in free-breathing with prospective gating for isotropic whole-lung MRI demonstrates an enhancement of 6.6 % in 8 healthy volunteers [48]. Oxygen-enhanced 3 D radial UTE showed a high concordance of signal enhancement and ventilation defects in 18 subjects within 15 days (ICC > 0.9), demonstrating the stability of the method as an alternative to hyperpolarized gas ventilation MRI [49].

The relative changes of the high UTE signal during the respiratory cycle can be further exploited, esp. when using an external reference to normalize lung signal intensities. Using this approach, the normalized expiratory signal in 17 asthma patients correlates well with the CT density ($r = 0.82$, $p = 0.004$) and ventilation defect percent in hyperpolarized gas MRI ($r = -0.67$, $p = 0.006$) [50]. Furthermore, the dynamic differences between

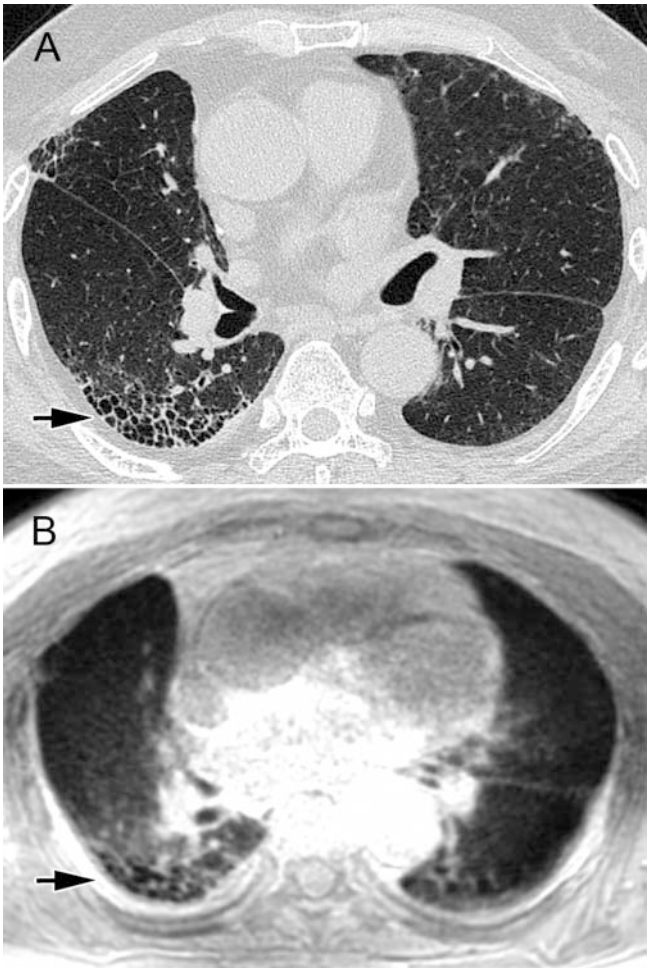

▶ **Fig. 4** 74-year-old male with usual interstitial pneumonia (UIP) as evidenced by honey combing on CT **A** and respiratory-gated pulmonary thin-section MR imaging with UTE at 96 µs on a 3 T system **B**. Note that UTE MRI is reconstructed in the end-expiration phase.

▶ **Abb. 4** 74 Jahre alter Mann mit usual interstitial pneumonia (UIP), erkennbar an den Honigwaben im CT **A** und in der Dünnschicht-3D-UTE mit Atemgating, gemessen bei 96µs auf einem 3T-Scanner **B**. Die UTE-Messung wurde in Exspiration rekonstruiert.

inspiration and expiration correlated well with CT density ($r = 0.71$, $p = 0.01$) as well as FEV1 % ($r = 0.61$, $p = 0.02$).

T2* mapping

T2* is an interesting parameter for gaining information on pathological changes on the mesostructure of the lung parenchyma. Multi-echo UTE sequences can be used to fit the exponential decay of T2* with points at a short TE [12, 13], demonstrating disease severity in smokers and patients with COPD as well as interstitial lung disease [51 – 53]. Since T2* is also affected by oxygen [46], it provides an additional tool for monitoring lung function through oxygen-enhanced imaging [29].

T1 mapping

The ability to increase the signal acquired from the lung parenchyma using UTE is also advantageous for T1 mapping showing

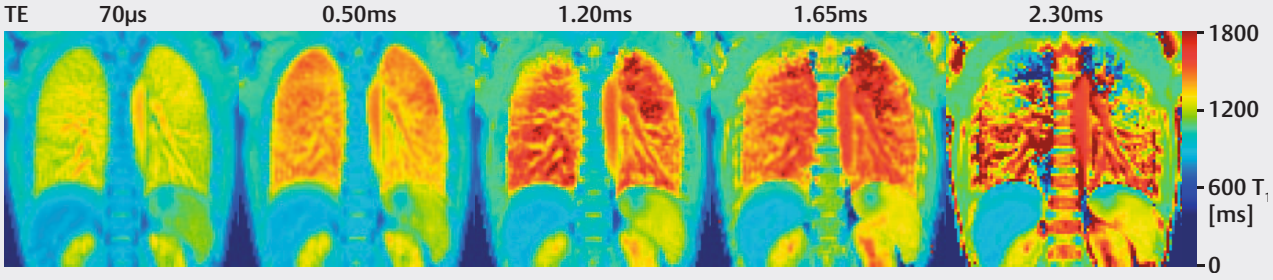

▶ **Fig. 5** Maps of observed T1 acquired using inversion recovery 2 D UTE at varying TEs in a healthy volunteer. T1 is found to increase with increasing TE.

▶ **Abb. 5** Parameterkarten des gemessenen T1, aufgenommen mittels einer Inversion-Recovery-Multi-Echo-2D-UTE in einem gesunden Probanden. Das gemessene T1 nimmt mit der Echo-Zeit zu.

differences in cystic fibrosis [54] and COPD [55] as well as the oxygen-induced reduction of T1, which also is smaller in COPD. The areas with reduced T1 nicely correlate with perfusion defects [55]. Probably, this reduction in T1 can be attributed to both hypoxic pulmonary vasoconstriction and the presence of emphysema [56]. While 3 D UTE requires very long total acquisition times, 2 D UTE can directly replace a conventional radial acquisition, though costing a factor of 2 in duration for the half-pulses. This also provides the option of measuring both T1 and T2* maps simultaneously by combining inversion recovery with a multi-gradient echo [29]. The parenchymal T1 depends on the TE it is measured at [57]: By using UTE, regional T1 was quantified at several TEs between 70 µs and 2.3 ms. Increasing the TE significantly prolonged T1 from 1060 to 1389 ms (▶ **Fig. 5**), thus opening an interesting perspective. This was attributed to the presence of protons in two water compartments (▶ **Fig. 1**). With both compartments having different compositions and thus magnetic properties, they also exhibit a different T1 and T2*. Thus, UTE-based quantification methods allow for a more differentiated look at the extravascular compartment, which is otherwise inaccessible to conventional quantification methods (▶ **Fig. 5**). T1 mapping of pulmonary perfusion may have the potential to further reduce the contrast agent burden, e. g. in CF [40], and may also enable tissue characterization in COPD and interstitial lung diseases.

UTE Perfusion MRI

UTE imaging of pulmonary perfusion with intravenous application of Gd-based contrast may increase both temporal resolution to roughly 1 s and spatial resolution to roughly 1.5 mm [58, 59]. Free-breathing 3 D UTE after Gd-contrast injection performs better in the detection of emboli especially in subsegmental arteries in an animal model for pulmonary embolism than the standard technique with a spoiled gradient-echo angiography, with CT serving as the standard of reference [60]. Non-contrast-dependent techniques are under development, such as a combination of arterial spin labelling with UTE showing promising sensitivity to lung perfusion changes under hyperoxia in rats measured at 7 T [61].

Conclusion

Recent developments in UTE-MRI are creating high expectations. It intrinsically addresses the three obstacles of lung MRI: Patient respiratory- and circulation-related motion, low proton density and the extremely fast signal decay due to susceptibility differences at air-tissue surfaces, by reducing the time gap between excitation and readout. Thus, it may overcome the old problem of the limited spatial resolution of MRI and may offer a radiation-free alternative to CT. Potential applications and initial studies in patients encompass, for example, nodule detection and precise morphological characterization, thus opening up new possibilities for no-dose lung cancer screening and nodule follow-up. In chronic obstructive airways diseases such as cystic fibrosis, the increased resolution helps to delineate fine intrapulmonary airways, mucus plugs and vasculature. Neonatal imaging benefits not only from the resolution which is required for identifying the small structures of the lung in neonates and preterm infants but also from the gating techniques compensating for respiratory movement. Since the original proposal of utilizing UTE in the lungs, the scanner hardware has only recently made employing such methods feasible on clinical MRI scanners. Subsequently, it may be the missing link between high-resolution imaging of lung structure and functional assessment that can further propel the implementation of MRI for routine lung imaging.

Conflict of Interest

The authors declare that they have no conflict of interest.

References

[1] Bergin CJ, Glover GH, Pauly JM. Lung parenchyma: magnetic susceptibility in MR imaging. Radiology 1991; 180: 845 – 848

[2] Wielpütz M, Kauczor HU. MRI of the lung: state of the art. Diagn Interv Radiol 2012; 18: 344 – 353

[3] Hansell DM, Bankier AA, MacMahon H et al. Fleischner Society: Glossary of Terms for Thoracic Imaging. Radiology 2008; 246: 697 – 722

[4] Wormanns D, Hamer OW. Glossary of Terms for Thoracic Imaging-German Version of the Fleischner Society Recommendations.

[5] Ohno Y, Koyama H, Yoshikawa T et al. Three-way comparison of whole-body MR, coregistered whole-body FDG PET/MR, and integrated whole-body FDG PET/CT imaging: TNM and stage assessment capability for non–small cell lung cancer patients. Radiology 2015; 275: 849 – 861

[6] Stahl M, Wielpütz MO, Graeber SY et al. Comparison of Lung Clearance Index and Magnetic Resonance Imaging for Assessment of Lung Disease in Children with Cystic Fibrosis. Am J Respir Crit Care Med 2017; 195: 349 – 359

[7] Bergin CJ, Pauly JM, Macovski A. Lung parenchyma: projection reconstruction MR imaging. Radiology 1991; 179: 777 – 781

[8] Pauly J, Conolly S, Nishimura D. Slice selective excitation for very short T2 species. SMRM

[9] Pauly J, Nishimura D, Macovski A. A k-space analysis of small-tip-angle excitation. J Magn Reson Imaging 1989; 81: 43 – 56

[10] Hatabu H, Alsop DC, Listerud J et al. T2* and proton density measurement of normal human lung parenchyma using submillisecond echo time gradient echo magnetic resonance imaging. Eur J Radiol 1999; 29: 245 – 252

[11] Hatabu H, Gaa J, Tadamura E et al. MR imaging of pulmonary parenchyma with a half-Fourier single-shot turbo spin-echo (HASTE) sequence. Eur J Radiol 1999; 29: 152 – 159

[12] Stock KW, Chen Q, Hatabu H et al. Magnetic resonance T2 measurements of the normal human lung in vivo with ultra-short echo times. Magnetic Resonance Imaging 1999; 17: 997 – 1000

[13] Yu J, Xue Y, Song HK. Comparison of lung T2* during free-breathing at 1.5 T and 3.0 T with ultrashort echo time imaging. Magn Reson Med 2011; 66: 248 – 254

[14] Biederer J, Beer M, Hirsch W et al. MRI of the lung (2/3). Why … when … how? Insights Imaging 2012; 3: 355 – 371

[15] Johnson KM, Fain SB, Schiebler ML et al. Optimized 3D ultrashort echo time pulmonary MRI. Magnetic Resonance in Medicine 2013; 70: 1241 – 1250

[16] Herrmann KH, Krämer M, Reichenbach JR. Time Efficient 3D Radial UTE Sampling with Fully Automatic Delay Compensation on a Clinical 3T MR Scanner. PLOS ONE 2016; 11: e0150371

[17] Marta T, Jan P, Andrea B et al. Multistage three-dimensional UTE lung imaging by image-based self-gating. Magnetic Resonance in Medicine 2016; 75: 1324 – 1332

[18] Delacoste J, Chaptinel J, Beigelman-Aubry C et al. A double echo ultra short echo time (UTE) acquisition for respiratory motion-suppressed high resolution imaging of the lung. Magn Reson Med 2018; 79: 2297 – 2305

[19] Jinil P, Taehoon S, Ho YS et al. A radial sampling strategy for uniform k-space coverage with retrospective respiratory gating in 3D ultrashort-echo-time lung imaging. NMR in Biomedicine 2016; 29: 576 – 587

[20] Glover GH, Pauly JM, Bradshaw KM. Boron-11 imaging with a three-dimensional reconstruction method. Journal of Magnetic Resonance Imaging 1992; 2: 47 – 52

[21] Duyn JH, Yang Y, Frank JA et al. Simple Correction Method for k-Space Trajectory Deviations in MRI. J Magn Reson Imaging 1998; 132: 150 – 153

[22] Hafner S. Fast imaging in liquids and solids with the Back-projection Low Angle ShoT (BLAST) technique. Magnetic Resonance Imaging 1994; 12: 1047 – 1051

[23] Madio DP, Lowe IJ. Ultra-fast imaging using low flip angles and fids. Magnetic Resonance in Medicine 1995; 34: 525 – 529

[24] Weiger M, Brunner DO, Dietrich BE et al. ZTE imaging in humans. Magnetic Resonance in Medicine 2013; 70: 328 – 332

[25] Dournes G, Grodzki D, Macey J et al. Quiet Submillimeter MR Imaging of the Lung Is Feasible with a PETRA Sequence at 1.5 T. Radiology 2015; 276: 258 – 265

[26] Grodzki DM, Jakob PM, Heismann B. Ultrashort echo time imaging using pointwise encoding time reduction with radial acquisition (PETRA). Magnetic Resonance in Medicine 2012; 67: 510 – 518

[27] Balcom BJ, Macgregor RP, Beyea SD et al. Single-Point Ramped Imaging withT1Enhancement (SPRITE). Journal of Magnetic Resonance, Series A 1996; 123: 131 – 134

[28] Pauly JM. Selective Excitation for Ultrashort Echo Time Imaging; John Wiley & Sons, Ltd; 2007

[29] Triphan SMF, Breuer FA, Gensler D et al. Oxygen enhanced lung MRI by simultaneous measurement of T1 and T2* during free breathing using ultrashort TE. Journal of Magnetic Resonance Imaging 2015; 41: 1708 – 1714

[30] Togao O, Tsuji R, Ohno Y et al. Ultrashort echo time (UTE) MRI of the lung: Assessment of tissue density in the lung parenchyma. Magnetic Resonance in Medicine 2010; 64: 1491 – 1498

[31] Lederlin M, Crémillieux Y. Three-dimensional assessment of lung tissue density using a clinical ultrashort echo time at 3 tesla: A feasibility study in healthy subjects. Journal of Magnetic Resonance Imaging 2014; 40: 839 – 847

[32] Biederer Jr, Schoene A, Freitag S et al. Simulated pulmonary nodules implanted in a dedicated porcine chest phantom: sensitivity of MR imaging for detection 1. Radiology 2003; 227: 475 – 483

[33] Sommer G, Tremper J, Koenigkam-Santos M et al. Lung nodule detection in a high-risk population: Comparison of magnetic resonance imaging and low-dose computed tomography. European Journal of Radiology 2014; 83: 600 – 605

[34] Burris NS, Johnson KM, Larson PEZ et al. Detection of small pulmonary nodules with ultrashort echo time sequences in oncology patients by using a PET/MR system. Radiology 2015; 278: 239 – 246

[35] Ohno Y, Koyama HH, Yoshikawa T et al. Standard-, Reduced- and No-Dose Thin-Section Radiological Examinations: Comparison of Capability for Nodule Detection and Nodule Type Assessment in Patients Suspected of Having Pulmonary Nodules. Radiology 2017. (in press)

[36] Wielpütz MO, Lee HY, Koyama H et al. Morphological Characterization of Pulmonary Nodules With Ultrashort TE MRI at 3T. Am J Roentgenol 2018; 210: 1216 – 1225

[37] Ohno Y, Koyama H, Yoshikawa T et al. Pulmonary high-resolution ultrashort TE MR imaging: Comparison with thin-section standard- and low-dose computed tomography for the assessment of pulmonary parenchyma diseases. Journal of Magnetic Resonance Imaging 2016; 43: 512 – 532

[38] Hahn AD, Higano NS, Walkup LL et al. Pulmonary MRI of neonates in the intensive care unit using 3D ultrashort echo time and a small footprint MRI system. Journal of Magnetic Resonance Imaging 2017; 45: 463 – 471

[39] Niwa T, Nozawa K, Aida N. Visualization of the airway in infants with MRI using pointwise encoding time reduction with radial acquisition (PETRA). J Magn Reson Imaging 2017; 45: 839 – 844

[40] Wielpütz MO, Eichinger M, Biederer J et al. Imaging of Cystic Fibrosis Lung Disease and Clinical Interpretation. Fortschr Röntgenstr 2016; 188: 834 – 845

[41] Eichinger M, Optazaite DE, Kopp-Schneider A et al. Morphologic and functional scoring of cystic fibrosis lung disease using MRI. European Journal of Radiology 2012; 81: 1321 – 1329

[42] Puderbach M, Eichinger M, Haeselbarth J et al. Assessment of morphological MRI for pulmonary changes in cystic fibrosis (CF) patients: comparison to thin-section CT and chest x-ray. Investigative radiology 2007; 42: 715 – 724

[43] Mall MA, Stahl M, Graeber SY et al. Early detection and sensitive monitoring of CF lung disease: Prospects of improved and safer imaging. Pediatric Pulmonology 2016; 51: S49 – S60

[44] Wielpütz MO, Puderbach M, Kopp-Schneider A et al. Magnetic Resonance Imaging Detects Changes in Structure and Perfusion, and Response to Therapy in Early Cystic Fibrosis Lung Disease. Am J Respir Crit Care Med 2014; 189: 956 – 965

[45] Edelman RR, Hatabu H, Tadamura E et al. Noninvasive assessment of regional ventilation in the human lung using oxygen-enhanced magnetic resonance imaging. Nat Med 1996; 2: 1196 – 1236

[46] Pracht ED, Arnold JFT, Wang T et al. Oxygen-enhanced proton imaging of the human lung using T2*. Magn Reson Med 2005; 53: 1193 – 1196

[47] Hemberger KR, Jakob PM, Breuer FA. Multiparametric oxygen-enhanced functional lung imaging in 3D. Magma (New York, NY) 2015; 28: 217 – 226

[48] Kruger SJ, Fain SB, Johnson KM et al. Oxygen-enhanced 3D radial ultrashort echo time magnetic resonance imaging in the healthy human lung. NMR in biomedicine 2014; 27: 1535 – 1541

[49] Zha W, Kruger SJ, Johnson KM et al. Pulmonary ventilation imaging in asthma and cystic fibrosis using oxygen-enhanced 3D radial ultrashort echo time MRI. J Magn Reson Imaging 2018; 47: 1287 – 1297

[50] Sheikh K, Guo F, Capaldi DP et al. Ultrashort echo time MRI biomarkers of asthma. J Magn Reson Imaging 2017; 45: 1204 – 1215

[51] Ohno Y, Koyama H, Yoshikawa T et al. T2* measurements of 3-T MRI with ultrashort TEs: capabilities of pulmonary function assessment and clinical stage classification in smokers. American Journal of Roentgenology 2011; 197: W279 – W285

[52] Ohno Y, Nishio M, Koyama H et al. Pulmonary MR imaging with ultrashort TEs: utility for disease severity assessment of connective tissue disease patients. European journal of radiology 2013; 82: 1359 – 1365

[53] Ohno Y, Nishio M, Koyama H et al. Pulmonary 3 T MRI with ultrashort TEs: Influence of ultrashort echo time interval on pulmonary functional and clinical stage assessments of smokers. Journal of Magnetic Resonance Imaging 2014; 39: 988 – 997

[54] Jakob PM, Wang T, Schultz G et al. Assessment of human pulmonary function using oxygen-enhanced T1 imaging in patients with cystic fibrosis. Magn Reson Med 2004; 51: 1009 – 1016

[55] Jobst BJ, Triphan SMF, Sedlaczek O et al. Functional Lung MRI in Chronic Obstructive Pulmonary Disease: Comparison of T1 Mapping, Oxygen-Enhanced T1 Mapping and Dynamic Contrast Enhanced Perfusion. PLoS ONE 2015; 10: e0121520

[56] Hopkins SR, Wielpütz MO, Kauczor HU. Imaging lung perfusion. J Appl Physiol 2012; 113: 328 – 339

[57] Triphan SMF, Jobst BJ, Breuer FA et al. Echo time dependence of observed T1 in the human lung. Journal of Magnetic Resonance Imaging 2015; 42: 610 – 616

[58] Bauman G, Johnson KM, Bell LC et al. Three-dimensional pulmonary perfusion MRI with radial ultrashort echo time and spatial–temporal constrained reconstruction. Magnetic Resonance in Medicine 2015; 73: 555 – 564

[59] Bell LC, Johnson KM, Fain SB et al. Simultaneous MRI of lung structure and perfusion in a single breathhold. Journal of Magnetic Resonance Imaging 2015; 41: 52 – 59

[60] Bannas P, Bell LC, Johnson KM et al. Pulmonary embolism detection with three-dimensional ultrashort echo time MR imaging: experimental study in canines. Radiology 2015; 278: 413 – 421

[61] Tibiletti M, Bianchi A, Stiller D et al. Pulmonary perfusion quantification with flow-sensitive inversion recovery (FAIR) UTE MRI in small animal imaging. NMR Biomed 2016; 29: 1791 – 1799